Design and experiment of the negative pressure adsorption Cartesian robot system for apple harvesting

Xiaofei Zhang[1], Yi Xun[1,2], Qinghua Yang[3,4*], Zhiheng Wang[1,2*]

(1. *College of Mechanical Engineering, Zhejiang University of Technology, Hangzhou 310032, Zhejiang, China*;
2. *Taizhou Key Laboratory of Advanced Manufacturing Technology, Taizhou Institute, Zhejiang University of Technology, Taizhou, 318014, Zhejiang, China*;
3. *College of Optical, Mechanical and Electrical Engineering, Zhejiang A & F University, Hangzhou 310032, Zhejiang, China*;
4. *The Collaborative Innovation Center for Intelligent Production Equipment of Characteristic Forest Fruits in Hilly and Mountainous Areas of Zhejiang Province, Zhejiang A & F University, Hangzhou 310032, Zhejiang, China*)

Abstract: To address the limitation of low harvesting efficiency in intelligent mechanized harvesting in standardized orchards, a negative pressure adsorption apple harvesting robot has been designed and developed. The robot is based on a Cartesian coordinate system and incorporates direct negative pressure adsorption picking combined with multi-stage buffering collection methods. Additionally, the proposed model pipeline integrates YOLOv8 and Segment Anything Model for precise apple picking point localization. Finally, field trials of the apple harvesting robot were conducted in a V-shaped layout apple orchard at Experiment and Demonstration Orchard at Tianping Lake. The experimental results showed an apple recognition rate of 90.54%, an overall harvesting success rate of 83.65%, an average picking efficiency of 4.83 s per fruit, and a damage rate of 13.61%. It demonstrates the potential of the robot in improving the efficiency and reliability of automated apple harvesting. At the same time, the results highlight the need to focus on enhancing the robustness of apple recognition algorithms under varying lighting conditions, and reducing apple damage rates by shortening the transport pipeline and optimizing the structure of the collection device. This study provides a promising solution for addressing global challenges in agricultural automation, offering insights into the future optimization of intelligent harvesting technologies.

Keywords: harvesting robot, apple, negative pressure adsorption, field trial.
DOI: 10.25165/j.ijabe.20251803.9308

Citation: Zhang X F, Xun Y, Yang Q H, Wang Z H. Design and experiment of the negative pressure adsorption Cartesian robot system for apple harvesting. Int J Agric & Biol Eng, 2025; 18(3): 145–153.

1 Introduction

Apples are one of the most popular fruits globally[1], and China is a major producer with the highest output in the world[2]. According to data from the National Bureau of Statistics of China in 2022, China's apple cultivation area was 1.956 million hm^2, yielding a staggering 47.572 million tons. While the cultivation area has decreased in recent years, production has shown a steady annual increase. Orchard harvesting is a highly seasonal, labor-intensive, and time-consuming process[3]. As modern agriculture moves towards intelligence and precision, replacing manual labor with intelligent robots for automated harvesting has become a major trend[4]. Achieving efficient and low-damage harvesting has always been the primary goal of automated harvesting systems[5]. Apples are predominantly grown in open fields and have a single annual harvest season, making apple picking a seasonal labor-intensive task. The shortage of rural labor has led to rising labor costs for manual harvesting, making the demand for harvest automation increasingly urgent[6].

In recent years, the research on automated apple harvesting robots has received widespread attention from numerous scholars[7,8]. Within this research, the design of end effectors for picking and the development of apple recognition algorithms have become two key technologies in this field. The end effectors of apple-picking robots mainly include pneumatic soft finger grippers, suction-based grippers, and a combination of both. In the research on pneumatic soft finger grippers, Pi et al.[9] proposed a pneumatically driven three-finger gripper that controls gripping and releasing apples through inflation and deflation. Chen et al.[10] proposed a three-finger soft claw inspired by the fin ray effect and combined it with a constant pressure feedback system to significantly enhance the safety of the soft fruit gripper. Li et al.[11] studied various picking modes of flexible three-finger end effectors and determined the optimal angle for the wrap-around pulling separation method. In the area of suction-based grippers, Wang et al.[12] designed a bionic, non-damaging apple-picking mechanical hand consisting of four suction cups, based on octopus predation mechanisms. The hand uses negative pressure to adhere to the apple, then separates the fruit stem using rotation and dragging, ultimately delivering the apple into a collection pipeline below to complete the harvesting process. In the development of grippers combining claws and suction, Zhang et al.[13] designed and developed a gripping mechanism that integrates a hollow flexible tube with three claws and has a swallowing function. This mechanism can precisely control the gripping force through force feedback, effectively reducing the damage rate to apples. Wang et al.[14] designed a pneumatic gripper consisting of four conical soft fingers and a suction cup, capable of

Received date: 2024-08-20 **Accepted date:** 2025-02-21
Biographies: Xiaofei Zhang, PhD candidate, research interest: agriculture robot, Email: zxf843390242@163.com; **Yi Xun**, PhD, Lecturer, research interest: robotics and automation, Email: xunyi@zjut.edu.cn.
***Corresponding author: Qinghua Yang**, PhD, Professor, research interest: agriculture robot. Zhejiang A&F University, Hangzhou 310023, China. Tel: +86-13067902888, Email: robot@zjut.edu.cn; **Zhiheng Wang**, PhD, Associate Professor, research interest: robot motion control, embedded system development and application, unmanned aerial vehicle remote sensing technology. Zhejiang University of Technology, Hangzhou 310023, China. Tel: +86-13777860388, Email: wzh232@zjut.edu.cn.

twisting and pulling operations to effectively separate apples from the tree. The common feature of these harvesting methods is that after the end effector contacts and secures the apple, additional operations such as rotation and dragging are typically required to detach the apple from the tree. Moreover, the harvested apples must be placed into a designated harvesting box or directly fall into a bottom collection box through an unloading process. The entire procedure involves both harvesting and collecting stages, which increases the time required to pick each apple.

In the research on apple recognition algorithms, in addition to using traditional machine learning methods for apple region segmentation[15], the performance of instance segmentation and object detection algorithms has significantly improved with the development of deep learning technologies. In terms of instance segmentation, Wang et al.[16] developed an improved version of the Mask Region-based Convolutional Neural Network (Mask RCNN), and Tang et al.[17] proposed an improved SOLOv2 high-precision apple instance segmentation method. Both methods demonstrated excellent apple target segmentation performance. In the field of object detection, due to their outstanding performance, YOLO series algorithms have been widely applied in fruit and vegetable recognition. Yan et al.[18] proposed a real-time apple harvesting recognition method based on an improved YOLOv5m, Zhou et al.[19] proposed a panoramic apple recognition method based on an improved YOLOv4 and threshold-based bounding box matching merging algorithm, and Wang et al.[20] developed a fast apple recognition and tracking method based on an improved YOLOv5 algorithm. All these methods achieved high recognition rates and efficiency. However, the rectangular bounding boxes generated by object detection algorithms sometimes do not perfectly align with the apple contours, leading to errors in locating the apple's center point, which affects harvesting accuracy. While instance segmentation algorithms can more accurately extract apple contours, they typically use polygon annotations that need to fit the target contour as closely as possible. Compared to the rectangular bounding box annotations in object detection, this significantly increases the labeling workload and is not conducive to expanding the dataset for different apple varieties in the future. Based on thorough research on apple harvesting robot end effectors and object detection algorithms, this paper proposes using a harvesting-integrated soft hose for direct adsorption as the end effector to improve harvesting efficiency. Additionally, combining YOLOv8 and Segment Anything Model (SAM) for apple visual recognition and segmentation aims to reduce the manual annotation time for image segmentation datasets.

This study aims to design and develop a Cartesian coordinate apple harvesting robot system based on negative pressure adsorption principles. The goal is to reduce the single-fruit harvesting time while ensuring a certain level of harvesting success rate, thereby effectively improving harvesting efficiency. First, this paper provides a detailed introduction to the overall system architecture of the apple harvesting robot, covering its mechanical structure, control system, and visual detection algorithm workflow. Then, field harvesting tests are conducted in a structured apple orchard, with a comprehensive explanation of relevant evaluation indicators. Finally, by analyzing the statistical harvesting results and comparing the key performance indicators of this system with those of other apple harvesting robots developed in recent years, the advantages and limitations of the proposed system are thoroughly examined, and future optimization directions are clearly identified.

2 System overall design

2.1 Orchard environment and robot workspace

Standardized apple orchards in China typically adopt "V-shaped", "Y-shaped", or "wall-shaped" structures with dwarf close-planting cultivation methods. These orchards are characterized by compact tree structures, open canopy space, and good ventilation and light penetration, which effectively enhance fruit quality and yield. Compared to traditional orchards, although standardized orchards require higher initial investment, their lower tree height and reduced fruit obstruction by branches and leaves make them more suitable for robotic harvesting, aligning with the needs of agricultural automation development[21]. As a result, this cultivation model has been strongly promoted by the Chinese government, along with corresponding policy support. The apple harvesting robot developed in this study is specifically designed for standardized apple orchards. The experimental site is located at the Tianping Lake Experimental Demonstration Base of the Shandong Fruit and Vegetable Research Institute, where the V-shaped tree planting method is adopted, as shown in Figure 1.

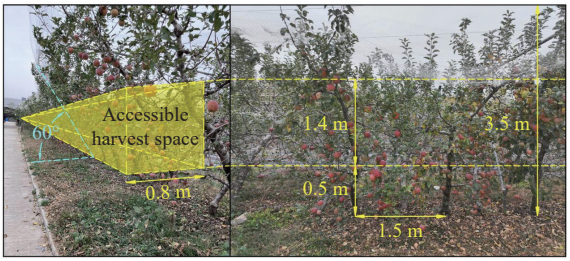

Figure 1 Planting structure and accessible harvest space of V-shaped apple orchard

The fruit trees boast a row spacing of approximately 3 m, a plant spacing of 1.5 m, and an average plant height of around 3.5 m[22]. The orchard primarily cultivates the Fuji apple variety, currently during its peak fruiting season, displaying predominantly red fruits. Noteworthy is the main stem's inclination at a 60-degree angle from left to right concerning the ground, stabilized by iron wires stretched horizontally across supporting steel pipes placed at intervals. Approximately 90% of the apples cluster beneath the main stem in a relatively dense arrangement, with the majority naturally hanging downwards due to gravity, concentrated below the canopy of branches and leaves. The experimental prototype's harvesting range is delimited by the Cartesian coordinate system track's length constraints, limiting access to the harvest space between 0.5-1.9 m in height and 0.8 m in depth, as delineated by the yellow area in Figure 1.

2.2 Robot overall structure

The apple harvesting robot uses a harvesting method based on the principle of negative pressure adsorption[23]. During the negative pressure harvesting operation, the end effector is connected to a vacuum high-pressure centrifugal fan via a pipeline. The fan extracts air from the negative pressure gas path to the external environment, generating a negative pressure source at the port of the end effector, which in turn generates an adsorption force to achieve the negative pressure picking function. As the end effector approaches the fruit, this negative pressure sucks the fruit into the flow channel. Compared to gripper methods, the method of direct negative pressure adsorption offers two main advantages: (1) It does not require precise image positioning or picking point positioning; as long as the end effector is close to a certain position around the

target fruit, negative pressure can suck the fruit into the channel. (2) It allows for continuous harvesting without the need for additional operations through end effector to place apples into the collection box, thereby reducing harvesting time for individual fruits and enhancing overall efficiency.

The 3D model and physical image of the apple harvesting robot are exhibited in Figure 2. This robot is mainly composed of a Cartesian mechanical structure, a pneumatic picking device, a buffer collection device, a vision system, a control system, and a mobile transport platform. Cartesian mechanical structure is used to transport the negative pressure adsorption end effector to the designated picking point position. The vision system, pneumatic picking device, and buffering collection device are respectively used for apple detection and positioning, picking, and collection. The control system coordinates the operation of various functional modules, including the fan and the robotic arm's movements. The mobile transport platform is used to install all components of the robot, which is towed by the tractor head to move on the inter-orchard road for continuous harvesting operations.

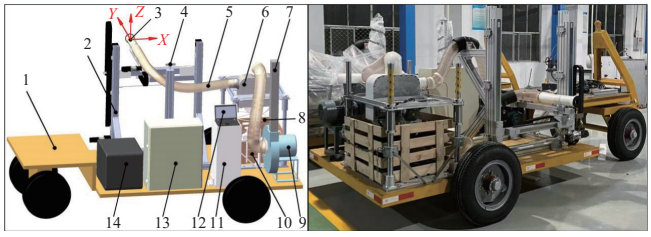

1. Mobile transport platform; 2. Cartesian robotic arm; 3. Negative pressure adsorption head; 4. Depth camera; 5. Hose; 6. Adsorption box; 7. Outlet pipe; 8. Rim; 9. High-pressure centrifugal fan; 10. Collection box; 11. Voltage regulator; 12. Computer; 13. Control cabinet; 14. Gasoline generator

Figure 2 3D model (left) and physical image (right) of the apple harvesting robot

2.2.1 Cartesian mechanical structure

In V-shaped apple orchards, apple positions can be described using a Cartesian coordinate system. The Cartesian robot system provides a rectangular workspace tailored to the fruit tree's shape. Cartesian coordinate robotic arms have the characteristics of simple structure, high dynamic performance, high motion accuracy, simple inverse kinematics scheme, and low cost[24,25]. Compared to articulated robots, Cartesian coordinate systems generate fewer steps during harvesting and reduce operational downtime, enhancing harvesting efficiency[26]. The Cartesian coordinate mechanical structure is composed of four standard linear modules forming an orthogonal gantry-style Cartesian coordinate structure (as shown in Component 2 of Figure 2). The *Z*-axis is driven by two synchronized linear modules, forming a high-load gantry structure with the *X*-axis modules. The *Z*-axis motor drives the *Z*-axis modules, which in turn move the *X*-axis module on the slider. The *Y*-axis module is mounted orthogonally to the *X*-axis. The *X*-axis motor moves the *X*-axis module, driving the slider and the *Y*-axis module. The *Y*-axis motor moves the *Y*-axis module. A negative pressure suction end effector is attached to the *Y*-axis, and the robotic arm moves the effector along the *X*-, *Y*-, and *Z*-axes to harvest apples.

2.2.2 End effector

The apple harvesting robot uses direct adsorption to harvest apples. Under the condition of constant fan power, the airflow output remains unchanged, and the intake airflow at the straight pipe inlet also remains constant. Based on the relationship between airflow rate, pipe inlet area, and airflow velocity, the intake velocity at the end effector's pipe inlet can be determined.

$$Q = S \cdot v \tag{1}$$

where, Q is the airflow rate of the centrifugal fan during operation. The centrifugal fan used in this harvesting robot has an airflow rate ranging from 2280 to 2504 m^3/h. S is the inlet area of the suction pipe, which is calculated based on the pipe diameter of 0.13 m, resulting in an inlet area of 0.0133 m^2. Therefore, the theoretical intake velocity v is determined to be in the range of 47.6-52.3 m/s. This velocity is significantly higher than the airflow velocity in a natural environment, allowing the effect of atmospheric airflow to be neglected.

Furthermore, according to the Bernoulli equation formula:

$$P + \rho g h + 1/2 \rho v^2 = C \tag{2}$$

where, P is the airflow pressure, Pa; ρ is the air density (1.225 kg/m^3); g is the gravitational acceleration (9.8 m/s^2); h is the height of the airflow, m; and C is a constant. From this, it can be inferred that under the assumption that the height of the end effector port remains unchanged during apple harvesting, as the inflow velocity increases, the pressure in the airflow region decreases. This phenomenon provides a theoretical basis for the increase in the adsorption force.

According to the adsorption force equation, it can be concluded that:

$$F = S \cdot (P_0 - P_1) = \pi (D/2)^2 (P_0 - P_1) \tag{3}$$

where, F is the picking adsorption force, N; P_0 is the standard atmospheric pressure, Pa; P_1 is the pipeline inlet pressure, Pa; and D is the pipe diameter, m. Therefore, the theoretical range of adsorption force is from 18.5 to 22.3 N.

Experiments conducted by horizontally pulling apples from the branches in the orchard showed that 95% of the apples required a minimum horizontal pulling force of less than 35 N to be harvested. However, in actual operation, the flow of gas within the pipeline is affected by frictional resistance, and the frictional losses reduce the airflow, thereby decreasing the adsorption force. For this apple harvesting robot, factors such as the length of the pipeline, surface roughness, and bends increase the frictional losses, thus reducing the actual adsorption force generated by the fan. Therefore, the required adsorption force for apple harvesting is clearly greater than the theoretical adsorption force of the negative pressure adsorption system. To address this, a solution is proposed: installing a silicone sleeve with an inner hole at the harvesting end of the end effector. The silicone sleeve not only enhances the adsorption force by reducing the inlet diameter but also serves as a cushioning layer to effectively reduce the direct impact between the apple and the pipe inlet.

During the harvesting operation, the blades of the centrifugal fan rotate and draw air outwards. In this process, the end effector gradually approaches the apple, the inlet area continually decreases, and the airflow velocity increases while maintaining a constant airflow rate. This leads to an increasing pressure difference on both sides of the apple, thus enhancing the picking suction as the pressure difference grows. When the suction reaches a certain level, the connection between the fruit stem and the branch breaks, and the apple is then sucked into the pipeline. However, in actual harvesting, due to potential positioning errors of the end effector, the surface of the apple may not fully fit the hole of the silicone sleeve. Positioning errors can affect the airflow velocity and its distribution, thereby influencing the magnitude and direction of the

suction force, ultimately impacting the effectiveness of the apple harvesting process.

To select the appropriate silicone sleeve with a suitable inner diameter, harvesting tests were conducted using silicone sleeves with inner diameters of 6 cm, 7 cm, 8 cm, and 9 cm. The results showed that the silicone sleeves with inner diameters of 8 cm and 9 cm experienced insufficient suction during the harvesting process. This was primarily due to positioning errors that caused the actual suction force to exceed the maximum suction force that the centrifugal fan could provide under full load. On the other hand, the silicone sleeve with an inner diameter of 6 cm caused apples, with an approximate diameter of 10 cm, to become stuck at the suction port and fail to enter the flow path smoothly. This was due to compression deformation when the silicone sleeve made contact with the apple surface, reaching its strain limit, causing the apple to become stuck in the inner hole of the silicone sleeve and preventing it from being successfully sucked in. Ultimately, the end effector of the apple harvesting robot used a silicone sleeve with an inner diameter of 7 cm, which demonstrated the best suction and harvesting performance during the tests. It effectively met the harvesting requirements for apples with diameters ranging from 6 cm to 12 cm.

2.2.3 Pneumatic picking and buffering collection device

The apple harvesting robot uses direct adsorption to harvest apples. As shown in Figure 3, the important components of the apple pneumatic picking and buffering collection device are displayed. During apple harvesting, the apple, which can be approximated as a nearly spherical object, has its center of mass directly used as a positioning point for the negative pressure adsorption[27].

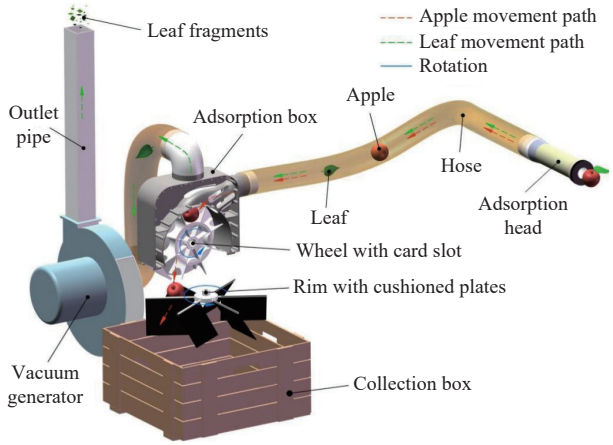

Figure 3 Schematic diagram of apple pneumatic picking and buffering collection device

The hose is made of polyurethane air duct material, known for its excellent elasticity, plasticity, and flexibility. It also has good extensibility, allowing it to adapt to the contraction caused by the movement of the robotic arm during the harvesting process. During the negative pressure adsorption harvesting operation, the leaves may be sucked into the hose along with the apples, and the separation of apples and leaves is completed in the adsorption box. The top of the adsorption box functions as the air outlet, the side as the air inlet, and the bottom as the apple outlet. Apples fall into the buffer collection device at the bend of the flow channel in this chamber due to centrifugal force, while leaves, being lighter, are drawn into the fan through the upper suction port, where they are chopped up before being discharged from the outlet pipe. The high-pressure centrifugal fan, installed in the vacuum generator device, serves as the negative pressure power source of the entire pneumatic harvesting device, and by adjusting its power, the magnitude of the negative pressure suction can be controlled, ensuring minimal energy consumption while meeting the requirements for apple harvesting.

The buffer collection device consists of a wheel with card slots, a rim with cushioned plates, and a collection box. The wheel with card slots is positioned below the adsorption box and is motor-controlled to rotate continuously. Cushioning cotton is placed in every slot. After passing through the adsorption box, apples fall into the slots on the wheel due to centrifugal force. As the wheel rotates, when the slot containing an apple reaches the fruit outlet, the apple falls onto the rim with cushioned plates due to gravity. The rim is lined with buffer cotton to prevent the apples from colliding. The flexible cushioned plates rotate along with the motor-driven rim, allowing the apples to roll into the collection box. The collection box is also lined with cushioning cotton to prevent the apples from colliding with the box frame. The wheel is designed as a rotating mechanism to prevent adjacent apples from colliding, while the rim is designed to rotate to ensure that the apples roll randomly into the collection box, preventing uneven accumulation inside the box.

2.2.4 Other components

The remaining components are shown in Figure 2. The host computer is a portable laptop, which issues picking commands through a visualized operation interface and is also used for program debugging. The vision system consists of a depth camera and a laptop, responsible for capturing image information and running vision algorithms, respectively. The entire apple harvesting robot system is powered by a gasoline generator, which converts gasoline into electrical energy to supply power to the high-pressure centrifugal fan, the motor group of the Delta coordinate robotic arm, and the host computer, among other electrical devices. All components of the aforementioned apple harvesting robot system are rationally arranged and installed on a carrier platform. Currently, the robot does not yet have autonomous driving capabilities and is towed by a manually driven tractor head to move through the apple orchard. However, future iterations of the system will explore the integration of autonomous navigation to further enhance operational efficiency. The following sections of this chapter will provide a detailed introduction to the control system and vision algorithm.

2.2.5 Workflow of apple harvesting robot

As shown in Figure 4, the workflow of the negative pressure adsorption apple harvesting robot includes: (1) The depth camera captures apple tree images, and the computer uses object detection algorithms to detect and position the apples in real time. (2) The detected apple coordinates, relative to the depth camera, are converted to the robot's global coordinate system, identifying which apples are accessible to the harvesting end effector. (3) Path planning for apple picking is completed based on the spatial positions of apples within the accessible harvest area. (4) The negative pressure adsorption picking head moves to the target positions in sequence, guided by the robot's XYZ motion, to pick each apple according to the task order. If an apple is not successfully harvested, secondary task planning and repeated attempts are made. After two failed attempts, the apple is abandoned, and the robot continues with the remaining tasks. (5) Apples are sucked into the adsorption box via the hose, where fruit and leaf separation occurs. Apples then fall into the fruit transfer wheel and roll into the collection box, while the leaves are directed to the crushing chamber and discharged via the outlet pipe.

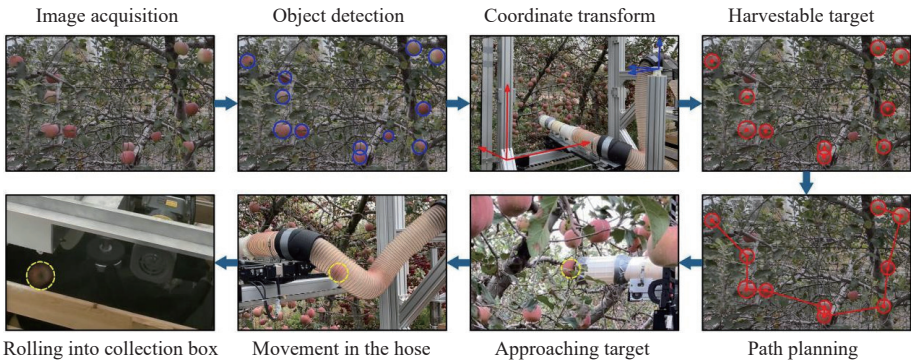

Figure 4 Workflow of negative pressure adsorption apple picking robot

2.3 Design of robot control system

The negative pressure adsorption apple picking robot designed in this paper utilizes a distributed control system. The computer is connected to the depth camera through a USB bus, and data exchange with the robot's motion controller is conducted through a CAN bus. The control system structure is illustrated in Figure 5. This paper employs a self-developed 3-axis robot motion controller that integrates Microchip's dsPIC33EV256GM106 digital signal controller and Shenzhen CMOSIC's TC6014 4-axis motion control chip to form a dual-core structure. The dsPIC digital controller primarily handles tasks such as CAN communication, I/O input and output, and control of the vacuum high-pressure centrifugal fan's frequency converter. The 3-axis interpolation motion of the robot is mainly managed by the TC6014. Real-time acquisition of apple image information relies on the Intel RealSense Depth Camera D435i, which is powered via USB. The physical image of the robot motion controller is shown in Figure 6.

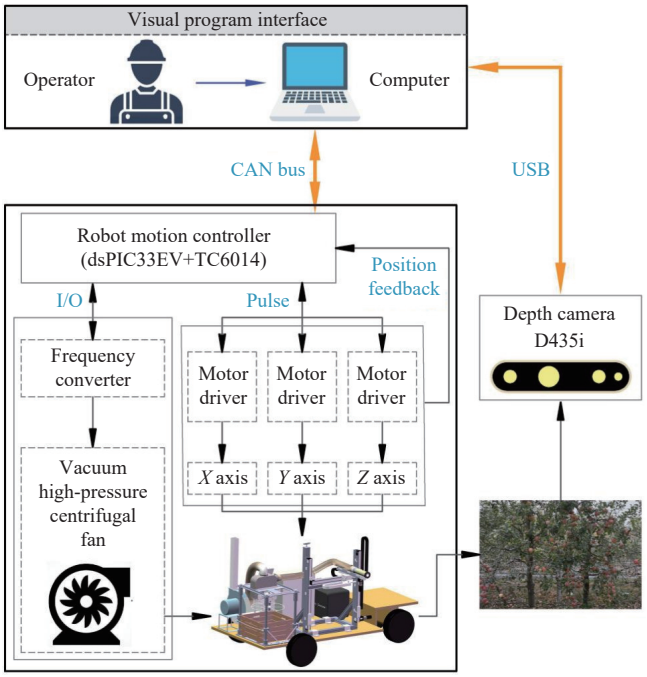

Figure 5 Schematic diagram of apple harvesting robot control system

During the apple harvesting process, apple image information captured by the depth camera is transmitted to the computer via a USB bus. The software on the upper computer uses image recognition algorithms to determine the spatial position of the target apple. It then performs coordinate transformation and inverse kinematics calculations to obtain the *XYZ* coordinates of the negative pressure adsorption picking head corresponding to the target apple's position. This coordinate information is transmitted to the robot's motion controller through the CAN bus. The motion controller manages the 3-axis movement of the picking robot, and real-time position information is fed back to the upper computer via the CAN bus to determine the precise movement of the picking head towards the target apple. The apple is then picked using the negative pressure adsorption system. Throughout the entire harvesting process, the negative pressure adsorption high-pressure centrifugal fan remains operational until the apple picking is completed.

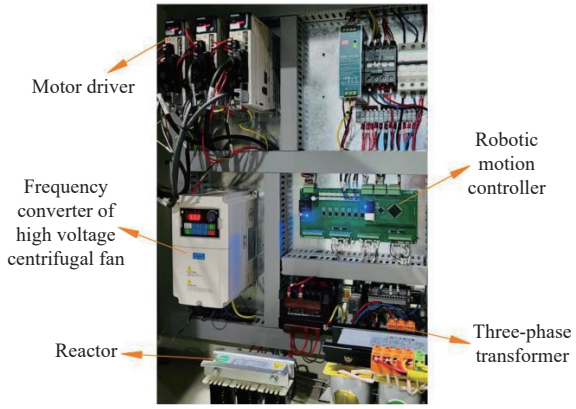

Figure 6 Physical picture of robot motion controller

2.4 Visual algorithm

The apple harvesting robot's visual algorithm combines YOLOv8 and SAM for apple target segmentation. YOLOv8 is a high-performance object detection algorithm widely used in agriculture, while SAM, known for its excellent segmentation performance, ease of deployment, and training-free nature, has gained attention in image segmentation[28]. By using YOLOv8's detection boxes as prompts for SAM, precise apple segmentation within these boxes is achieved. This fusion eliminates the need for complex contour annotations, reducing annotation costs and improving efficiency, especially when expanding datasets for different lighting and apple varieties.

On October 25, 2023, at the V-shaped apple tree plantation in Tai'an, Shandong, a cart equipped with RealSense D435i and an onboard computer captured 204 images of mature apples. After reviewing these images, 120 were labeled using Make Sense software, resulting in 3518 apples labeled. The training set had 100 images with 2781 labels, and the validation set had 20 images with 737 labels. Data augmentation techniques, including flipping, noise addition, and brightness adjustment, were used to address challenges like lighting and leaf obstruction.

The robot used YOLOv8n for apple detection, with a deep learning framework built on Windows 11, Python 3.8.18, Cuda11.7, and Pytorch 1.13.1. The primary hardware was a Dell G16 laptop with an Intel® Core™ i7-12700H CPU, NVIDIA GeForce RTX 3070 Ti GPU, and 32GB RAM. The model was trained with a batch size of 16 for 300 epochs using the Stochastic Gradient Descent algorithm. The best result achieved a precision of 0.893, recall of 0.849, and an average precision (AP@50) of 0.914.

To demonstrate the visual algorithm process, the original image (Figure 7a) is first processed with YOLOv8n to detect apples (Figure 7b). Detection boxes are fed into SAM for segmentation, producing apple masks (Figure 7c). The apple contours are extracted using OpenCV's "cv2.findContours" (Figure 7d), and the minimum circumcircle for each apple contour and its corresponding center are determined using "cv2.minEnclosingCircle" (Figures 7e and 7f). Red dots in Figure 7f show the localization points of all detected apples.

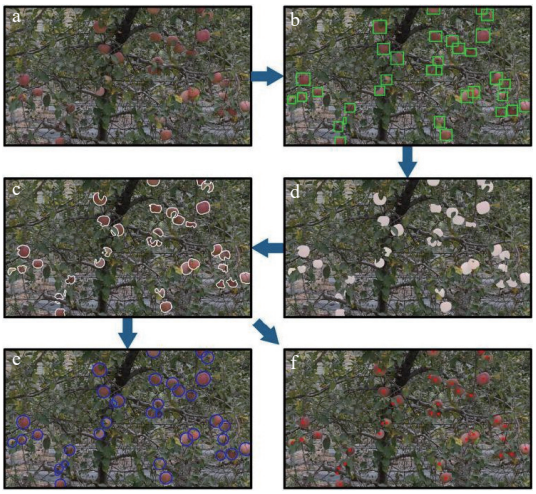

a. Original image; b. Object detection based on YOLOv8n; c. Mask segmentation based on SAM; d. Mask contour extraction; e. Minimum circumcircle fitting of contour; f. Apple positioning points in the image

Figure 7 Visual algorithm flow chart

3 Harvesting experiment

3.1 Orchard field experiment

From November 2-4, 2023, multiple rounds of on-site application tests of the negative pressure adsorption apple harvesting Cartesian coordinate robot were conducted at the Experiment and Demonstration Orchard at Tianping Lake (117°01′12″E, 36°13′01″N), as shown in Figure 8.

Figure 8 Harvesting robot on-site application test

In a standard V-shaped apple orchard, 10 apple trees were selected as test subjects, with a total of 404 apples counted within the accessible harvesting space. The specific data are shown in Table 1. A depth camera was mounted on a 1.5-meter-high profile to ensure a good field of view. The harvesting robot, towed by a manually driven tractor, moved between rows of trees and harvested apples on the right side of each tree. After the tests, the results were analyzed, with the vehicle's trajectory kept parallel to the rows to maximize the number of apples within the accessible range.

Table 1 Apple harvest data statistics

Type	1	2	3	4	5	6	7	8	9	10	Total
N_a	42	36	48	35	31	43	40	45	33	51	404
N_d	38	33	43	32	29	39	36	40	30	45	365
N_h	35	29	39	28	28	36	32	38	28	44	337
N_r	48	41	53	40	36	45	44	47	39	49	442
N_u	29	27	35	25	25	32	31	30	23	32	289
$T(s)$	154	143	192	155	104	168	176	182	143	210	1627

According to the flowchart shown in Figure 9, the number of apples corresponding to the relevant harvesting evaluation indicators for each test tree is obtained in sequence. Before the harvest test, the number of apples within the accessible harvesting space N_a of ten fruit trees and the number of apples successfully detected by the vision system within the accessible harvesting space N_d were manually counted. After completing the harvesting test, the number of apples successfully harvested from each of the ten apple trees N_h into the collection box were manually counted. Real-time video recording was used to measure the time T taken for the robot to harvest apples within the accessible harvesting space of each fruit tree (excluding the time required for manually moving the apple harvesting robot between different harvesting points), and to record the total number of harvesting operations times N_r performed on a single fruit tree. Finally, the apples harvested by the robot are grouped according to the label of each tree and placed in a well-ventilated area at room temperature for 24 hours. After that, experienced apple quality inspectors from the orchard assess the apples on-site, based on the standards for first-grade Fuji apples, specifically regarding punctures, bruises, and abrasions. The specific regulations are as follows: the apple skin should be free of punctures, the total area of bruises or abrasions should not exceed 1 cm^2, and the largest individual bruise or abrasion should not exceed 0.5 cm^2. Apples that do not meet the first-grade Fuji apple quality requirements for punctures, bruises, or abrasions are defined as damaged apples. The number of damaged apples N_u under each tree label is then counted and recorded. The detailed results of the field harvesting experiment are presented in Table 1.

3.2 Evaluation indicators for harvesting experiments

According to the flowchart shown in Figure 9, the evaluation indicators for the harvesting experiments of the negative pressure adsorption Cartesian robot system for apple harvesting are calculated, as detailed below. The apple recognition rate N_d/N_a is the ratio of the number of apples detected by the vision system within the accessible harvest space to the actual number of apples in that space. It is used to assess the detection performance of the harvesting robot's vision system. The overall harvest success rate of apples N_h/N_a refers to the ratio of the number of apples successfully harvested to the actual number of apples within accessible harvest space. It measures the overall effectiveness of the harvesting robot system. The success rate of apple harvesting N_h/N_d refers to the ratio of the number of apples successfully harvested to the number of apples detected by the vision system within accessible harvest space. It evaluates the performance of the mechanical and control system of the harvesting robot's end effector. The apple damage rate $(N_h-N_u)/N_h$ is the ratio of the difference between the number of successfully harvested apples and the number of apples without surface damage inside the collection box to the number of

successfully harvested apples. It evaluates the possibility of damage to apples caused by the harvesting process and corresponding harvesting devices. The redundancy harvesting rate $(N_r - N_d)/N_d$ of apples is the ratio of the difference between the total number of harvesting operations times and the number of apples detected by the vision system within the harvestable range to the number of apples detected by the vision system within the harvestable range. It is used to evaluate the accuracy of harvesting operations. The corresponding evaluation indicators were calculated based on the results of each apple tree harvest experiment, and the results were plotted in the line chart on the right side of Figure 9. The horizontal axis represents the fruit tree numbers from 1 to 10, the vertical axis represents the ratio of each evaluation indicator, and the dashed line indicates the average value of each indicator.

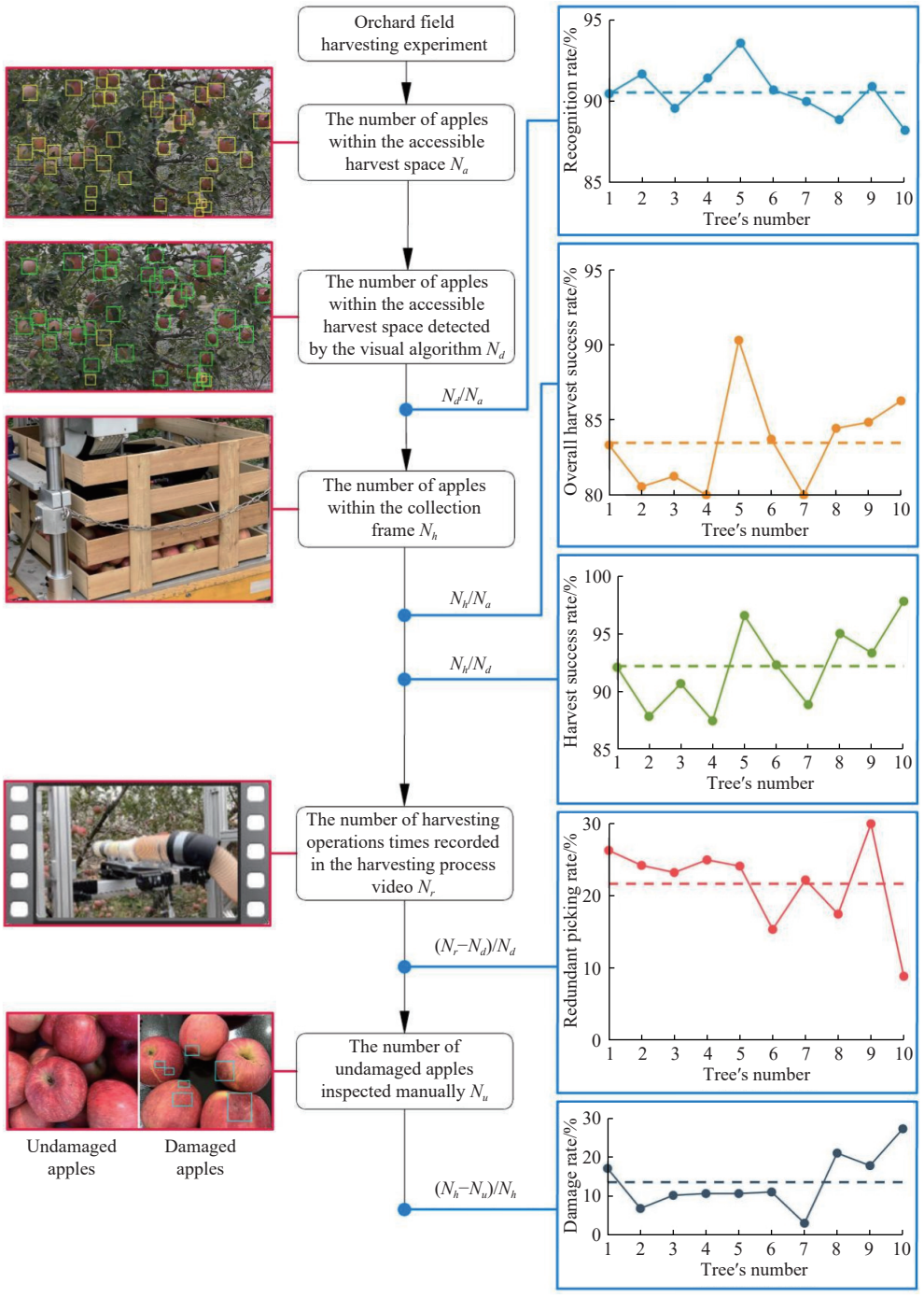

Figure 9 Data acquisition and processing flowchart for harvesting evaluation indicators

In addition to the five evaluation indicators mentioned above, the average harvesting time per apple $\bar{t}$ is calculated by dividing the total time T consumed by the actual total number of harvested apples N_h. This indicator is used to assess the harvesting efficiency of robots. These six evaluation indicators for the negative pressure adsorption Cartesian coordinate apple harvesting robot provide a comprehensive assessment of the robot's performance and offer clearer directions for subsequent performance improvements.

4 Experimental results and analysis

In the apple harvesting robots developed over the past three years, three key indicators—overall harvesting rate, single fruit harvesting time, and fruit damage rate—were statistically analyzed, as listed in Table 2. The harvesting methods are categorized into claw-based gripping harvesting and vacuum-based suction harvesting. The vacuum-based method is further divided into

separated harvesting and integrated harvesting. In the separated vacuum-based harvesting, Hu et al.[29]and Zhang et al.[30] used a vacuum device to generate negative pressure to attach the apple to the nozzle (with the nozzle diameter smaller than the apple's diameter). The apple was then picked from the tree by rotating (rotation) and pulling (pulling), and finally placed into a collection bin. The integrated harvesting method proposed in this paper uses negative pressure generated by a centrifugal fan to directly suck the apple into the pipeline, where it passes through a multi-stage buffering device before entering the collection bin. Compared to other harvesting methods, this vacuum suction-based integrated harvesting method allows the robot to immediately proceed to the next harvesting task after picking one apple, without occupying additional robot working time during the collection process, thus significantly improving harvesting efficiency. Therefore, the single fruit harvesting time for this method was shorter, averaging 4.83 s.

Table 2 Comparison of harvesting performance of different apple harvesting robots

Research team	Harvesting method	Overall harvest success rate	Harvesting time (s/per fruit)	Damage rate
Bu et al. 2022[31]	Grasp and release	82.93%	15.53	~0%
Hu et al. 2022[29]	Vacuum suction and rotation-pull	47.37%	4.00	~0%
Zhang et al. 2023[30]	Vacuum suction and drop	82.40%	6.00	~6.00%
Huang et al. 2024[32]	Grip and rotation	76.97%	7.29	0.43%
Our team, 2024	Direct negative pressure suction	83.65%	4.83	13.61%

Additionally, the apple harvesting robot demonstrated a high overall harvesting success rate of 83.65%. This success is attributed to the high tolerance for positioning errors in this harvesting method, as well as its ability to effectively harvest apples even when slightly obstructed by branches or leaves. The actual average recognition accuracy for apples was 90.54%, significantly lower than the generally required 95%. In the future, apple recognition accuracy should be improved by expanding the dataset to cover various lighting conditions and optimizing the algorithm structure to enhance recognition accuracy under occlusion conditions. The average fruit harvesting success rate was 92.36%. Approximately 5% of apples could not be harvested due to branch occlusion, as branches obstructed the harvesting head from approaching the apple's surface, resulting in insufficient suction force and leading to harvesting failure (as shown in Figure 10a). Additionally, apples that were too large in diameter (as shown in Figure 10b) could not pass through the harvesting head, while apples that were too small in diameter (as shown in Figure 10c) could not effectively cover the holes at the end of the buffering layer, leading to insufficient suction force and preventing harvesting.

Regarding the apple damage rate, this robot's harvesting method had the highest damage rate at 13.61%. In other methods, the apple was well-buffered during contact with the end effector or collection device, resulting in a lower damage rate. The primary cause of damage was collision with the transport pipeline wall, which was approximately 2 meters long with two bends. Future improvements could involve reducing the number of bends and shortening the pipeline to decrease damage. Additionally, when two adjacent apples were harvested simultaneously (as shown in Figure 10d), the risk of collision increased in the pipeline and grading device. Future work should focus on optimizing the buffering collection device for continuous harvesting.

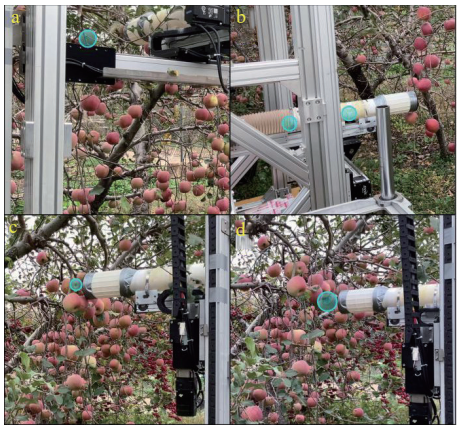

a. Too many branches and leaves obstructed the suction head, preventing harvest; b. Negative pressure suction pulled in two adjacent apples, increasing collision risk; c. Apples smaller than 5 cm could not block the silicone sleeve hole, leading to insufficient suction force; d. Apples larger than 12 cm got stuck at the suction opening.

Figure 10 Some problems encountered in the harvesting experiment

In addition to the above indicators, the redundant picking rate of the apple harvesting robot was 21.69%. Redundant picking primarily occurs when apples are severely obstructed by branches or when the apple's size is too large or too small, causing two failed picking attempts. Apart from the aforementioned failures, another situation arose where a small amount of branches and leaves obstruct the target apple. In such cases, the negative pressure suction head first absorbed the branches and leaves to clear the obstruction, and the apple was successfully harvested in the second attempt.

To avoid repeated failed harvesting attempts, the likelihood of success should be assessed using visual algorithms, considering factors like obstruction level and apple diameter. Abandoning unharvestable apples can reduce redundant attempts and improve efficiency. Additionally, misidentifying branches and leaves as apples increases invalid picks, mainly due to dataset issues. Excessive samples of obstructed apples may cause feature confusion and model overfitting. Future annotation should better address heavily obstructed apples. In the current trial, the suction head retracts along the *Y*-axis after each pick to avoid branch collisions but lacks consideration of branch distribution. Optimizing the harvesting path based on apple positions and branch distribution could further reduce harvesting time, making it a key focus for future efficiency improvements.

5 Conclusions

In response to the automated harvesting needs of standardized apple orchards in China, a negative pressure adsorption Cartesian coordinate apple harvesting robot system suitable for structured planting modes was designed. On-site tests conducted in apple orchards with a V-shaped planting pattern showed that the object detection and image segmentation algorithms based on Yolov8 and Segment Anything Model achieved an apple recognition rate of 90.54% within the accessible harvesting space. Compared to claw-type apple harvesting robots and the separate picking and collecting vacuum adsorption apple harvesting robots, this integrated picking and collecting negative pressure adsorption apple harvesting robot achieved a higher overall harvesting success rate (83.65%) and faster individual apple harvesting speed (4.83 s, including harvesting failures but excluding robot movement time between

trees), but had a higher damage rate of 13.61%. In the future, the damage rate will be reduced by shortening the apple transport pipeline and optimizing the collection method. Additionally, the object detection method will be improved under severe branch and leaf occlusion and complex lighting conditions to enhance apple recognition. Furthermore, considering the effects of branch occlusion and apple diameter, the apple harvesting path will be further optimized to improve overall harvesting efficiency.

Acknowledgement

This study was financially supported by China's Central Guiding Local Technology Development Special Fund Project (Grant No. ZYYD2025CG21), the Zhejiang Science and Technology Plan Project-National Key Research and Development Program of China (Grant No. 2019C03075), "Leading Goose" Research and Development Program Subproject of Zhejiang (Grant No. 2022C02021), and Xinjiang Boshiran Intelligent Agricultural Machinery Co., Ltd. (Grant No. KYY-HX-20210639).

[References]

[1] Cheng J L, Guo W C, Zhang Z Y, Zeng S C, Wang Z W. Optical properties of 'Gala'(Malus pumila) apple pulp and their relationship with internal quality. Infrared Physics & Technology, 2022; 123: 104210. DOI: 10.1016/j.infrared.2022.104210

[2] Zhao X, Cao G H, Zhang P F, Ma Z H, Zhao L J, Chen J N. Dynamic analysis and lightweight design of 3-DOF apple picking manipulator. Transactions of the CSAM, 2023; 54(7): 88–98. (in Chinese) DOI: 10. 6041/j. issn. 1000-1298.2023.07.009

[3] Chen Q, Yin C K, Guo Z L, Wang J P, Zhou H P, Jiang X S. Current status and future development of the key technologies for apple picking robots. Transactions of the CSAE, 2023; 39(4): 1–15. (in Chinese) DOI: 10.11975/j.issn.1002-6819.202209041

[4] Fei Z H, Vougioukas S G. A robotic orchard platform increases harvest throughput by controlling worker vertical positioning and platform speed. Computers and Electronics in Agriculture, 2024; 218: 108735. DOI: 10.1016/j.compag.2024.108735

[5] Liu C L, Gong L, Yuan J, Li Y M. Current status and development trends of agricultural robots. Transactions of the CSAM, 2022; 53(07): 1–22, 55. (in Chinese) DOI: 10.6041/j. issn. 1000-1298.2022.07.001

[6] Zhao Y X, Wan X F, Duo H X. Review of rigid fruit and vegetable picking robots. Int J Agric & Biol Eng, 2023; 16(5): 1–11. DOI: 10.25165/j.ijabe.20231605.8120

[7] Jia W K, Zhang Y, Lian J, Zheng Y J, Zhao D, Li C J. Apple harvesting robot under information technology: A review. International Journal of Advanced Robotic Systems, 2020; 17(3). DOI: 10.1177/1729881420925310

[8] Barbosa Júnior M R, Santos R G, Sales L A, Oliveira L P. Advancements in Agricultural Ground Robotsfor Specialty Crops: An Overview of Innovations, Challenges, and Prospects. Plants, 2024; 13(23): 3372. DOI: 10.3390/plants13233372

[9] Pi J, Liu J, Zhou K H, Qian M Y. An octopus-inspired bionic flexible gripper for apple grasping. Agriculture, 2021; 11(10): 1014. DOI: 10.3390/agriculture11101014

[10] Chen K W, Li T, Yan T J, Xie F, Feng Q C, Zhu Q Z, Zhao C J. A soft gripper design for apple harvesting with force feedback and fruit slip detection. Agriculture, 2022; 12(11): 1802. DOI: 10.3390/agriculture12111802

[11] Ji W, He G Z, Xu B, Zhang H W, Yu X W. A new picking pattern of a flexible three-fingered end-effector for apple harvesting robot. Agriculture, 2024; 14(1): 102. DOI: 10.3390/agriculture14010102

[12] Wang M R, Yan B, Zhang S H, Fan P, Zeng P Z, Shi S Q, Yang F Z. Development of a novel biomimetic mechanical hand based on physical characteristics of apples. Agriculture, 2022; 12(11): 1871. DOI: 10.3390/agriculture12111871

[13] Zhang Z, Zhou J, Yi B Y, Zhang B H, Wang K. A flexible swallowing gripper for harvesting apples and its grasping force sensing model. Computers and Electronics in Agriculture, 2023; 204: 107489. DOI: 10.1016/j.compag.2022.107489

[14] Wang X, Kang H W, Zhou H Y, Au W, Wang M Y, Chen C. Development and evaluation of a robust soft robotic gripper for apple harvesting. Computers and Electronics in Agriculture, 2023; 204: 107552. DOI: 10.1016/j.compag.2022.107552

[15] Fan P, Lang G D, Guo P J, Liu Z J, Yang F Z, Yan B, Lei X Y. Multi-feature patch-based segmentation technique in the gray-centered RGB color space for improved apple target recognition. Agriculture, 2021; 11(3): 273. DOI: 10.3390/agriculture11030273

[16] Wang D, He D. Fusion of Mask RCNN and attention mechanism for instance segmentation of apples under complex background. Computers and Electronics in Agriculture, 2022; 196: 106864. DOI: 10.1016/j.compag.2022.106864

[17] Tang S X, Xia Z L, Gu J N, Wang W B, Huang Z D, Zhang W H. High-precision apple recognition and localization method based on RGB-D and improved SOLOv2 instance segmentation. Frontiers in Sustainable Food Systems, 2024; 8: 1403872. DOI: 10.1016/j.compag.2023.107952

[18] Yan B, Fan P, Wang M R, Shi S Q, Lei X Y, Yang F Z. Real-time Apple Picking Pattern Recognition for Picking Robot Based on Improved YOLOv5m. Transactions of the CSAM, 2022; 53(09): 28–38, 59. (in Chinese) DOI: 10.6041/j. issn. 1000-1298.2022.09.003

[19] Zhou G H, M S, Liang F F. Recognition of the apple in panoramic images based on improved YOLOv4 model. Transactions of the CSAE, 2022; 38(21): 159–168. (in Chinese) DOI: 10.11975/j.issn.1002-6819.2022.21.019

[20] Wang J X, Su Y H, Yao J H, Liu M, Du Y R, Wu X, Huang L, Zhao M H. Apple rapid recognition and processing method based on an improved version of YOLOv5. Ecological Informatics, 2023; 77: 102196. DOI: 10.1016/j.ecoinf.2023.102196

[21] Yan B, Li X M. RGB-D camera and fractal-geometry-based maximum diameter estimation method of apples for robot intelligent selective graded harvesting. Fractal and Fractional, 2024; 8(11): 649. DOI: 10.3390/fractalfract8110649

[22] Yang S, Wang H R, Wang G P, Wang J Z, Gu A G, Xue X M, Chen R. Effects of Seaweed-Extract-Based Organic Fertilizers on the Levels of Mineral Elements, Sugar–Acid Components and Hormones in Fuji Apples. Agronomy, 2023; 13(4): 969. DOI: 10.3390/agronomy13040969

[23] Yang S Z, Ji J C, Cai H X, Chen H. Modeling and force analysis of a harvesting robot for button mushrooms. IEEE Access, 2022; 10: 78519–78526. DOI: 10.1109/ACCESS.2022.3191802

[24] Bottin M, Cipriani G, Tommasino D, Doria A. Analysis and control of vibrations of a Cartesian cutting machine using an equivalent robotic model. Machines, 2021; 9(8): 162. DOI: 10.3390/machines9080162

[25] D'Imperio S, Berruti T M, Gastaldi C, Soccio P. Tunable Vibration Absorber Design for a High-Precision Cartesian Robot. Robotics, 2022; 11(5): 103. DOI: 10.3390/robotics11050103

[26] Au C K, Barnett J, Lim S H, Duke M. Workspace analysis of Cartesian robot system for kiwifruit harvesting. Industrial Robot: the international journal of robotics research and application, 2020; 47(4): 503–510. DOI: 10.1108/IR-12-2019-0255

[27] Feng Q C, Zhao C J, Li T, Chen L P, Guo X, Xie F, Xiong Z C, Chen K W, Liu C, Yan T J. Design and test of a four-arm apple harvesting robot. Transactions of the CSAE, 2023; 39(13): 25–33. (in Chinese) DOI: 10.11975/j.issn.1002-6819.202305114

[28] Kirillov A, Mintun E, Ravi N, Mao H Z, Rolland C, Gustafson L, Xiao T T, Whitehead S, C. Berg A, Lo W Y, Dollár P, Girshick R. Segment anything. Proceedings of the IEEE/CVF International Conference on Computer Vision, 2023; 4015-4026. DOI: 10.48550/arXiv.2304.02643

[29] Hu G R, Chen C, Chen J, Sun L J, Sugirbay A, Chen Y, Jin H L, Zhang S, Bu L X. Simplified 4-DOF manipulator for rapid robotic apple harvesting. Computers and Electronics in Agriculture, 2022; 199: 107177. DOI: 10.1016/j.compag.2022.107177

[30] Zhang K X, Lammers K, Chu P Y, Li Z J, Lu R F. An automated apple harvesting robot—From system design to field evaluation. Journal of Field Robotics, 2024; 41(7): 2384–2400. DOI: 10.1002/rob.22268

[31] Bu L X, Chen C K, Hu G R, Sugirbay A, Sun H X, Chen J. Design and evaluation of a robotic apple harvester using optimized picking patterns. Computers and Electronics in Agriculture, 2022; 198: 107092. DOI: 10.1016/j.compag.2022.107092

[32] Huang W L, Miao Z H, Wu T, Guo Z W, Han W K, Li T. Design of and experiment with a dual-arm apple harvesting robot system. Horticulturae, 2024; 10(12): 1268. DOI: 10.3390/horticulturae10121268